

## Constraining sterile neutrinos with a low energy beta-beam

Sanjib K. Agarwalla,<sup>1,\*</sup> Patrick Huber,<sup>1,†</sup> and Jonathan M. Link<sup>1,‡</sup>

<sup>1</sup>*Department of Physics, IPNAS, Virginia Tech, Blacksburg, VA 24061, USA*

### Abstract

We show that a low energy beta-beam facility can be used to search for sterile neutrinos by measuring the disappearance of electron anti-neutrinos. This channel is particularly sensitive since it allows to use inverse beta decay as detection reaction; thus it is free from hadronic uncertainties, provided the neutrino energy is below the pion production threshold. This corresponds to a choice of the Lorentz  $\gamma \simeq 30$  for the  ${}^6\text{He}$  parent ion. Moreover, a disappearance measurement allows the constraint of sterile neutrino properties independently of any CP violating effects. A moderate detector size of a few 100 tons and ion production rates of  $\sim 2 \cdot 10^{13} \text{ s}^{-1}$  are sufficient to constrain mixing angles as small as  $\sin^2 2\theta = 10^{-2}$  at 99% confidence level.

---

\*Electronic address: sanjib@vt.edu

†Electronic address: pahuber@vt.edu

‡Electronic address: jonathan.link@vt.edu

## I. INTRODUCTION

A large number of experiments have now convincingly demonstrated that active neutrinos, *i.e.* left handed neutrinos which interact via W and Z exchange, can change their flavor. More recently, KamLAND [1] is providing direct evidence for neutrino oscillations. The oscillation of three<sup>1</sup> active neutrinos describes the global neutrino data very well, see *e.g.* [3]. The fact that neutrinos oscillate implies that at least two of the mass eigenstates have a non-zero mass. Most models to accommodate massive neutrinos introduce right handed neutrinos, *i.e.* states which do not couple to W and Z bosons. These right handed neutrinos can either directly provide a Dirac mass term or they mediate the seesaw mechanism [4]. In the latter case, the right handed neutrino tends to be very heavy with  $m_R \sim 10^{12} - 10^{15}$  GeV. However, in the most general scenario there is a 6x6 mass matrix whose entries are essentially unknown. To obtain the physical neutrino masses at scales below the electroweak phase transition this mass matrix has to be diagonalized and its eigenvalues are the neutrino masses relevant for low energy observations. Since the entries of the mass matrix are not known it can give rise to any spectrum of eigenvalues and thus neutrino masses. The need to describe the oscillation of three active neutrinos implies that *at least* three eigenvalues have to be of  $\mathcal{O}(1\text{ eV})$  or less. However, there can be 0 – 3 additional small eigenvalues corresponding to light neutrino states, which due to the Z decay width bound would have to be sterile. Thus, we conclude that sterile neutrinos are theoretically well motivated by the observation of neutrino mass. Furthermore, we see that there can be one or more sterile neutrinos which are light enough to play a role in neutrino oscillations. Note, that all these considerations are entirely independent of any experimental claims to have seen sterile neutrinos, like, for example, the one by LSND [5].

Interpretations of the LSND claim in terms of only sterile neutrino oscillation have failed [6]. The remaining models for explaining LSND, see *e.g.* [7], are viable explanations of the data only because of the fact that direct tests of LSND, like MiniBooNE [8], employ a different baseline or energy, while the ratio  $L/E$  is close to the original experiment. Therefore, the status of LSND can only be settled by experiments using the same  $L$  and the same  $E$ .

Light sterile neutrinos have a large number of phenomenological consequences. Most notably, they would contribute to the energy density of the Universe and being highly relativistic, they would act as hot dark matter. This allows us to use various cosmological data sets to put severe bounds on the mass of the light sterile neutrinos of order 1 eV [9]. Among other things, these bounds rely on the sterile neutrinos being in equilibrium with the surrounding thermal bath. Since they are sterile, the only interaction<sup>2</sup> they have is via mixing with active neutrinos. Thus the cosmological mass bounds only apply if the mixing with active neutrinos is sufficiently large. Even very weakly mixing sterile neutrinos can have visible effects in astrophysics [10–13] or Big Bang nucleosynthesis [14, 15]. However, these small mixings can be beyond the reach of terrestrial experiments.

In this work we explore how well sterile neutrinos can be constrained by a dedicated

---

<sup>1</sup> We know from the invisible decay width of the Z boson [2], that there are 3 active neutrinos with  $m < m_Z/2$ .

<sup>2</sup> besides gravity, which however is far too small for this purpose.

oscillation experiment based on a low energy beta-beam facility. For other physics which can be studied using a low energy beta-beam, *e.g.* see [16]. The proposed experiment is a disappearance experiment and will be sensitive to  $\Delta m^2 = 0.5 - 50 \text{ eV}^2$  and can probe mixing angles as small as  $\sin^2 2\theta = 10^{-3} - 10^{-2}$ . The oscillation probability for our purposes is a two flavor  $\bar{\nu}_e \rightarrow \bar{\nu}_s$  oscillation and the survival probability of  $\bar{\nu}_e$  is given by

$$P_{\bar{e}\bar{e}} = 1 - \sin^2 2\theta \sin^2 \frac{\Delta m^2 L}{4E}. \quad (1)$$

Note, that this parametrization is phenomenologically complete, in the sense that the electron neutrino disappearance probability in any  $3 + N$  neutrino scenario can be parametrized like given in equation 1. For instance, in the common  $3 + 1$  scheme,  $\sin^2 2\theta = 4|U_{e4}|^2(1 - |U_{e4}|)^2$ , for small  $\sin^2 2\theta$  this can be inverted and we find  $|U_{e4}|^2 \simeq 1/4 \sin^2 2\theta$ . On the other hand,  $\sin^2 2\theta_{\text{SBL}} = 4|U_{e4}|^2|U_{\mu 4}|^2$ , where  $\theta_{\text{SBL}}$  is the angle constrained by short baseline appearance experiments like LSND or MiniBooNE.  $|U_{\mu 4}|^2$  is constrained by  $\nu_\mu$  disappearance experiments like CDHS and found to be smaller than 0.1 and thus, a bound on  $\sin^2 2\theta$  becomes bound on  $\sin^2 2\theta_{\text{SBL}} \leq 0.1 \sin^2 2\theta$ , see *e.g.* reference [17].

The most sensitive experiments in this mass range looking for the disappearance of  $\bar{\nu}_e$  have been the reactor neutrino experiments: Bugey [18] and Chooz [19]. The Bugey bound is valid in the range  $\Delta m^2 = 0.1 - 1 \text{ eV}^2$  and it can constrain  $\sin^2 2\theta$  below  $5 \cdot 10^{-2}$ . The bound from Chooz is  $\sin^2 2\theta \simeq 10^{-1}$  for  $\Delta m^2 > 0.01 \text{ eV}^2$ .

## II. EXPERIMENTAL SETUP

The concept we propose here is based on using a pure  $\bar{\nu}_e$  beam from the beta decay of completely ionized radioactive ions circulating inside a storage ring. The Lorentz boost  $\gamma$  of these ions will be chosen such that the resulting  $\bar{\nu}_e$  have an energy below the pion production threshold. In this case, the by far most likely reaction is inverse beta decay on free protons. In this experiment we have an accurate theoretical understanding of the neutrino flux, spectrum and cross section. The detector will be placed so close to the neutrino source that oscillation will happen *within* the detector itself. Thus the different parts of the detector will effectively act as near and far detector. This allows the cancellation of most systematical errors in a similar fashion as in modern reactor neutrino experiments. A concept exploiting several oscillation maxima inside one detector has been proposed using very low energy neutrinos from a stationary ( $\gamma = 1$ ) radioactive source inside the LENS detector. This concept is called LENS-Sterile and more details and sensitivity estimates can be found in [20].

### A. Beta-beam

In [21], the idea of using beta decay of exotic nuclei to produce well defined neutrino beams was introduced. The basic observation is, that if a beta decaying nucleus is moving with a

Lorentz  $\gamma \gg 1$ , the isotropic<sup>3</sup> neutrino emission will be collimated into a beam. A beta-beam facility consists of four parts: isotope production, ionization, acceleration and storage ring. Obviously, only isotopes which have the right lifetime are suitable for a beta-beam; they need to be long lived enough to allow sufficient time for beam formation and acceleration. On the other hand they need to be short lived enough to produce a reasonable neutrino flux. Isotopes with lifetimes around 1 s turn out to be the most suitable [21]. The isotope we consider here is  ${}^6\text{He}$ , which beta decays with a half life of 0.81 s and has an end-point energy  $E_0 = 4.02 \text{ MeV}$ . The production of exotic isotopes is a well understood technology which has been developed for studies of nuclear physics; for a review, see *e.g.* [22].  ${}^6\text{He}$  is most efficiently produced by the ISOL method in conjunction with a so called converter: a proton beam impinges on a primary spallation target, the converter, which in turn produces neutrons. These neutrons then hit a Beryllium target where the  ${}^6\text{He}$  is produced. Helium, being a noble gas, easily escapes the Beryllium target. With this approach, production rates,  $p$ , of  $2 \cdot 10^{13} \text{ ions s}^{-1}$  are achievable [23].

However, the number of ions which can actually be injected into the storage ring is significantly smaller and we will present a simplified estimate of this number. First of all, there will be decay losses, which are incurred mostly while the ions are still at very low  $\gamma$ . The fraction of ions lost to decays depends on the ratio of the beta lifetime and the time required for ionization, beam formation and initial acceleration. We assume that this time is dominated by the cycle time,  $t_c$ , of the accelerator and that the decay losses happen while waiting for the accelerator. Secondly, there will be the usual losses from beam handling and acceleration,  $\epsilon_a$ . We assume  $\epsilon_a = 0.5$ . The number of ions which can be accelerated in each cycle,  $n_c$ , is given by

$$n_c = \epsilon_a p \tau \left(1 - e^{-\frac{t_c}{\tau}}\right). \quad (2)$$

Also, during acceleration a number of ions will decay and we assume that the  $\gamma$  rises linearly from injection into the accelerator till to the point where the ions leave the accelerator. The number of ions after acceleration,  $n_a$ , is

$$n_a = n_c \gamma^{-\frac{t_c}{(\gamma-1)\tau}}. \quad (3)$$

The rate of ions,  $n_i$ , which can be injected into the storage ring is  $n_i = n_a/t_c$ . Note, that this expression has the correct asymptotic behavior:  $\lim_{t_c \rightarrow 0} n_i = p$ . Typical cycle times range from around 8 s (CERN PS) down to about 1.8 s (FNAL main injector). Taking  $\gamma = 30$ , this yields a range for  $n_i = (0.3 - 3) \cdot 10^{12} \text{ s}^{-1}$ . Note, that these numbers are based on current technology and no special effort for optimization has been made. Therefore a rate of  $3 \cdot 10^{12} \text{ s}^{-1}$  ions injected into the storage is conservative and will be our default setup (corresponding to an accelerator like the FNAL main injector). The issue of luminosity and useful ions for beta beams has been studied in much more detail and the resulting parameters can be found at [24]. In this considerably more realistic study an injection rate of  $1.5 \cdot 10^{12} \text{ s}^{-1}$  is found, albeit at  $\gamma = 100$ . Given, that at lower  $\gamma$  the losses in acceleration are less, our simplistic estimate agrees very well with this number. Furthermore, we assume

---

<sup>3</sup> Beta decay is naturally isotropic for nuclei with initial spin of 0 and for the other nuclei the decay is isotropic for an ensemble of ions with unpolarized nuclear spins.

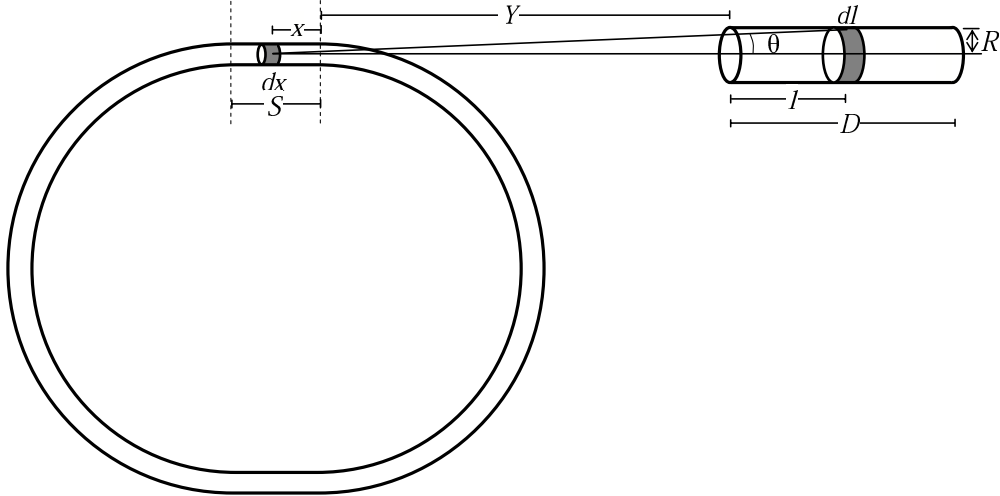


**FIG. 1:** Schematic of the detector and storage ring.

that the beta-beam complex operates for  $1.6 \cdot 10^7$  s per calendar year and our experiment runs for a total of five years.

In order to compute the fraction of useful decays, *i.e.* those decays which happen in the straight section of the storage ring, we need to specify the geometry of the storage ring. We consider a magnetic field  $B = 5$  T inside the storage ring. Taking  $\gamma = 30$  this yields magnetic radius  $\rho = 56$  m for the  ${}^6_2\text{He}^{++}$  ion. The useful fraction,  $f$ , of decays then is given by the ratio of the length of the straight section,  $S$ , to the overall circumference of the ring.

$$f = \frac{S}{2S + 2\pi\rho}. \quad (4)$$

In an ordinary beta-beam experiment the goal is to maximize  $f$  by choosing  $S$  to be very large. This is possible because the baseline,  $L$ , is much larger than  $S$ ,  $L \gg S$ . Thus the storage ring, despite its large size, can be approximated as a point source. Here, however, we will consider the case where  $S$  and  $L$  are of the same order,  $S \sim L$ . If the goal is to measure oscillation we need to have an accurate determination of  $L/E$ . Obviously, a lower bound on the uncertainty on  $L/E$  is given by  $S$  itself. Therefore, we would like to have  $S$  small enough as to maintain the oscillatory signature. On the other hand,  $S$  should be as large as possible to have the largest possible event rate. As we will discuss later in detail, a good choice of  $S = 10$  m. Thus, we obtain  $f = 2.7\%$ . Note, that due to very short straight section, the majority of decays will happen in the arcs; this will lead to considerable energy deposition in the magnets, which may exceed the heat load or radiation tolerance of the magnets. This problem needs further study, but is outside of the scope of this work.

## B. Event rate calculation

Figure 1 shows a schematic of the setup we consider. In this scheme we will have a cylindrical detector whose symmetry axis is aligned with the straight section of the storage ring. The free parameters are (see figure 1): the length of the straight section ( $S$ ), the distance between the front end of the storage ring and the front end of the cylindrical

detector ( $Y$ ), the radius ( $R$ ) and the length ( $D$ ) of the detector. In the following, we will derive a general expression for the neutrino event rate as a function of these free parameters.

Neglecting the small Coulomb corrections to the beta-spectrum<sup>4</sup>, the lab frame neutrino beta-beam flux per unit length of the straight section in units of  $\text{sr}^{-1} \text{MeV}^{-1} \text{s}^{-1} \text{m}^{-1}$  emitted at an angle  $\theta$  with the beam axis is described by

$$\phi^{Near}(E, \theta) = \frac{1}{4\pi} \frac{g}{m_e^5 f} \frac{1}{\gamma(1 - \beta \cos \theta)} (E_0 - E^*) E^{*2} \sqrt{(E_0 - E^*)^2 - m_e^2}, \quad (5)$$

where  $m_e$  is the electron mass,  $E_0$  is the electron total end-point energy and  $E^*$  is the rest frame energy of the emitted neutrino<sup>5</sup>.  $f$  is the phase space factor associated with the beta decay of the nucleus.  $\gamma$  is the Lorentz boost such that  $E^* = \gamma E(1 - \beta \cos \theta)$ ,  $E$  being the neutrino energy in the lab frame.  $g \equiv N_0/S$  is the number of useful decays per unit time per unit length of the straight section.

To calculate the resulting number of events in a cylindrical detector of radius  $R$  and length  $D$  aligned with the beam axis it is necessary to integrate over the length  $S$  of the straight section of the storage ring and the volume of the detector. Here we assume that the beam is perfectly collinear and has no transverse extension<sup>6</sup>. The un-oscillated event rate in a detector placed at a distance  $Y$  from the storage ring is given by

$$\frac{dN}{dt} = n\varepsilon \int_0^S dx \int_0^D d\ell \int_0^{\theta'} d\theta 2\pi \sin \theta \int_{E_{min}}^{E'} dE \phi^{Near}(E, \theta) \sigma(E), \quad (6)$$

where

$$\tan \theta'(x, \ell) = \frac{R}{Y + x + \ell} \quad \text{and} \quad E' = \frac{E_0 - m_e}{\gamma(1 - \beta \cos \theta)}. \quad (7)$$

Note, that the baseline, relevant for oscillations, is  $L = Y + x + \ell$ . Here,  $n$  represents the number of target nucleons per unit detector volume,  $\varepsilon$  is the detector efficiency which is taken to be unity in our calculation.  $E_{min}$  denotes the energy threshold for our detection method. We work with a threshold of 25 MeV which ensures that our events are well above the backgrounds.  $\sigma(E)$  stands for the inverse beta decay reaction cross section [25], which is the predominant reaction channel at the considered energies. Figure 2 shows the resulting un-oscillated event rates for  $S = 10$  m,  $Y = 50$  m,  $R = 3.6$  m and  $D = 28.7$  m. This corresponds to a detector mass of 1 kton.

### C. Statistical Analysis

For our statistical analysis we use the so called pull approach as used in [26, 27]. We bin our data in  $L/E$  into bins of equal width. The  $\chi^2$  function is defined as

$$\chi_{\bar{\nu}_e \rightarrow \bar{\nu}_e}^2 = \min_{\xi_s} \left[ 2 \sum_{i=1}^n (\tilde{y}_i - N_i^{ex} - N_i^{ex} \ln \frac{\tilde{y}_i}{N_i^{ex}}) + \xi_s^2 \right], \quad (8)$$

<sup>4</sup> We checked that these corrections are negligible for our purposes.

<sup>5</sup> Quantities without the ‘\*’ refer to the lab frame.

<sup>6</sup> Note, that the beam size is of order  $10^{-2}$  m, whereas all other length scales are of order  $\sim 10$  m.

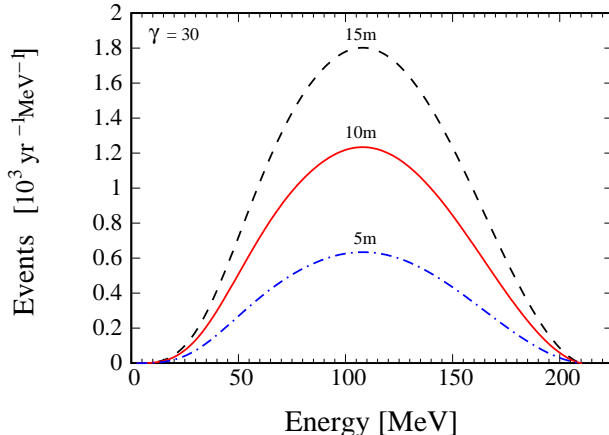


**FIG. 2:** The un-oscillated event rate as a function of neutrino energy. The event rate has been calculated including all geometrical effects and with a luminosity of  $3 \cdot 10^{12}$  ions  $s^{-1}$ . The different lines show the result for different values of the length of the straight section,  $S$ , as indicated by the labels next to each line.

where  $n$  is the total number of  $L/E$  bins and

$$\tilde{y}_i(\{\Delta m^2, \sin^2 2\theta\}, \{\xi_s\}) = N_i^{th}(\{\Delta m^2, \sin^2 2\theta\}) [1 + \pi^s \xi_s] , \quad (9)$$

where  $N_i^{th}(\{\Delta m^2, \sin^2 2\theta\})$  is the predicted number of events in the  $i$ -th  $L/E$  bin for a set of oscillation parameters  $\Delta m^2$  and  $\sin^2 2\theta$ . The quantity  $\pi^s$  in Eq. (9) is the systematic error on the normalization of our signal. We have taken  $\pi^s = 1\%$  to estimate the performance of our standard set up. The quantity  $\xi_s$  is the “pull” due to the systematical error on signal. In Eq. (8),  $N_i^{ex}$  corresponds to the data of the experiment. Since there is no data yet, this number of observed signal events in the detector has been computed for the case of no neutrino oscillation. We assume that our setup is background free, see also section II E. Even if this assumption were violated we do not expect this to affect our sensitivity since the background will not be able to mimick the oscillatory behavior of the signal as shown in figure 3.

#### D. Optimization of the geometry

The goal is to obtain an experimental configuration which has optimal sensitivity to the disappearance of  $\bar{\nu}_e$  corresponding to a mass squared difference  $\Delta m^2 = 1 - 10 \text{ eV}^2$ . For this optimization we fixed the detector mass at 1 kton, thus  $D$  is entirely determined by  $R$  or *vice versa*. We tested values of the detector distance  $Y = \{30, 50, 70, 90\}$  m. We studied variations in  $\gamma$  from 20 – 35. This range was chosen to stay below or close to the pion production threshold. We also changed the detector radius from 3.5 – 4.5 m. We found that within those options the configuration with

$$\begin{aligned} \gamma &= 30 & S &= 10 \text{ m} \\ L &= 50 \text{ m} & D &= 28.7 \text{ m} \end{aligned} \quad (10)$$

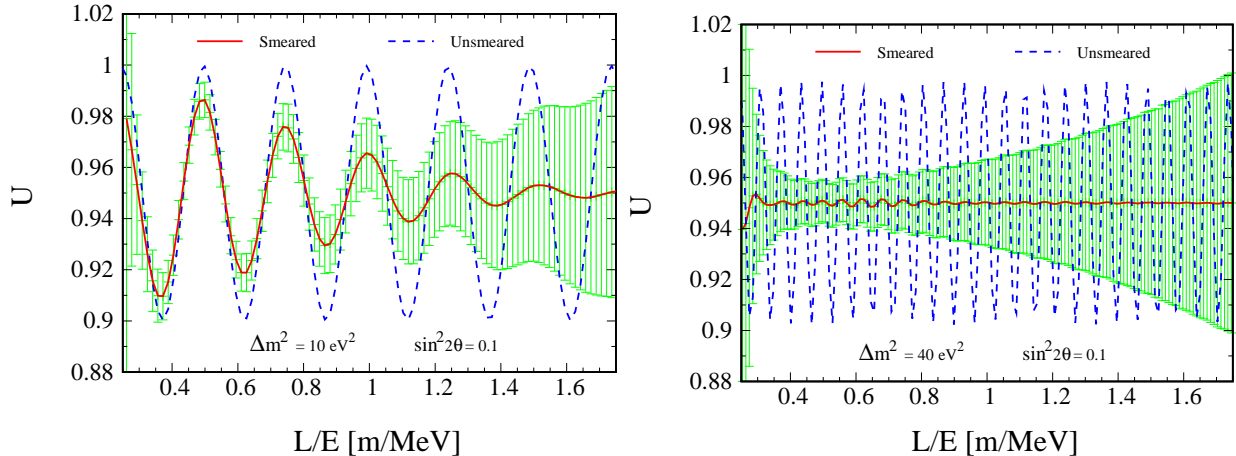


**FIG. 3:** This figure shows the ratio of oscillated to un-oscillated events as a function of the reconstructed  $L/E$ . In left panel,  $\Delta m^2 = 10 \text{ eV}^2$  and in right panel  $\Delta m^2 = 40 \text{ eV}^2$ . The value of mixing term  $\sin^2 2\theta = 0.1$ . The red (solid) line includes all geometrical effects and the detector resolution, whereas the blue (dashed) line assumes a point source of neutrinos.

is optimal. It is easy to see that for an average baseline  $(S/2 + Y + D/2) \simeq 70 \text{ m}$  and a  $\gamma = 30$  we have the first oscillation maximum around  $\Delta m^2 \simeq 2 \text{ eV}^2$ . Note, that the parameters in equation 10 yield both a baseline and energy close to the ones of LSND.

Using these numbers, figure 3 shows the resulting ratio of oscillated to un-oscillated event rates for two different values of  $\Delta m^2$  as a function of the reconstructed  $L/E$ . The blue line assumes that the neutrinos are all generated at in one point in the middle of the straight section. The red line fully accounts for all the geometry effects. Clearly, for  $\Delta m^2 = 10 \text{ eV}^2$  (left hand panel), several oscillation periods can be resolved. A comparison between the amplitudes of those periods allows to cancel systematics to a large extent (see also, figure 4). At  $\Delta m^2 = 40 \text{ eV}^2$  (right hand panel) only an average suppression can be observed and the sensitivity is entirely determined by the achievable systematic errors.

### E. Detector

The detector we envisage is essentially similar to the MiniBooNE detector [28], however with a cylindrical shape. The important background will all be beam based, since beam-off backgrounds will be well measured and cosmic ray events can be tagged with high efficiency as was done in similar near surface experiments [28]. The beam energy has been selected to be below threshold for pion production, therefore there are few channels available for neutrino interactions. Only charged current quasi-elastic scattering on carbon and electron elastic scattering can mimic the signal of the inverse beta decay primary positron. These event types will experience the same disappearance rates due to oscillations, but the neutrino energy reconstructed under the inverse beta decay hypothesis would be systematically less than the true neutrino energy. At these energies the cross sections for these background interactions are smaller by at least an order of magnitude, so any effect they might have on the measured oscillation parameters, in particular  $\sin^2 2\theta$  would be at most 10%, and they

can be accounted for and corrected.

To further reduce the impact of these beam based backgrounds, the detector should be optimized for the detection of inverse beta decay. Typically this is done by tagging the primary positron with the free neutron capture in delayed coincidence with a mean lifetime of  $\sim 200 \mu\text{s}$  in undoped organic scintillator. However, observing the 2.2 MeV gamma ray from neutron capture on hydrogen can be a significant challenge in a detector tuned to see events in the 50 to 200 MeV range. Additionally, the long delay time will put several beam bunches between the primary and secondary events and will therefore increase the probability of false tags. Adding gadolinium to the scintillator would help somewhat by increasing the tag energy to 8 MeV and reducing the capture time to  $\sim 30 \mu\text{s}$ . Nevertheless, even if the neutron tag was highly efficient, at least some of the quasi-elastic events on carbon will also have a correlated neutron capture tag. Another possibility is to design the detector to be sensitive to the positron direction. We expect the elastic scattering events to be peaked in the very forward direction, while the quasi-elastic carbon events will have a much broader angular distribution. The angular distribution of the hydrogen inverse beta decay events will fall somewhere in between. Sensitivity to the angular distribution can be achieved by reducing the scintillation light to a point where Čerenkov light can be distinguished.

To achieve an energy resolution of 10% or better over the 50 to 200 MeV range should be possible with a photo-cathode coverage of 10% if we assume approximately equal parts Čerenkov and scintillation light [28]. Position and timing resolutions, needed to correlate events with beam bunches, should be achievable at the half meter and 10 ns level. With a bunch spacing of 100 ns or greater, this resolution would provide sufficient space between bunches to demonstrate the rejection of non-beam backgrounds. At this level of detector resolution the  $L/E$  uncertainty is fully dominated by the unknown production point in the straight section of the decay ring.

### III. RESULTS

Figure 4 shows the obtainable sensitivity in the  $\sin^2 2\theta - \Delta m^2$  plane at 99% CL. Our default configuration is shown as red solid line in both panels. The setup proposed here improves on the existing limit for  $\Delta m^2 \geq 0.2 \text{ eV}^2$ . In the range  $1 \text{ eV}^2 < \Delta m^2 < 10 \text{ eV}^2$  the improvement is one order of magnitude or better. The left hand panel shows how the sensitivity changes with varying the length of the straight section. A longer straight section (dash-dotted line) implies a large fraction of useful decays and thus better statistics. At the same time the  $L/E$  resolution is reduced. As a result the sensitivity extends to smaller mixing angles (higher statistics) but at smaller  $\Delta m^2$  (resolution). The analogous arguments holds also for a shorter straight section (dashed line), which yields smaller statistics but better resolution. This improves sensitivity to  $\Delta m^2 > 10 \text{ eV}^2$ . Thus the length of the straight section can effectively be used to tune the experiment to the desired range of  $\Delta m^2$  and it can be envisaged to have running periods with different straight section lengths within the same setup. The right hand panel shows variations of the systematic error  $\pi^s$  as defined in equation 9. Again our default setup with  $\pi^s = 0.01$  is shown as red, solid line. At very small  $\pi^s = 0.001$  the sensitivity (dash-dotted blue line) becomes essentially independent of  $\Delta m^2$ , once the first oscillation maximum can be observed. Note, that this very small value of  $\pi^s = 0.001$  probably is not attainable in a real experiment. For more realistic values of

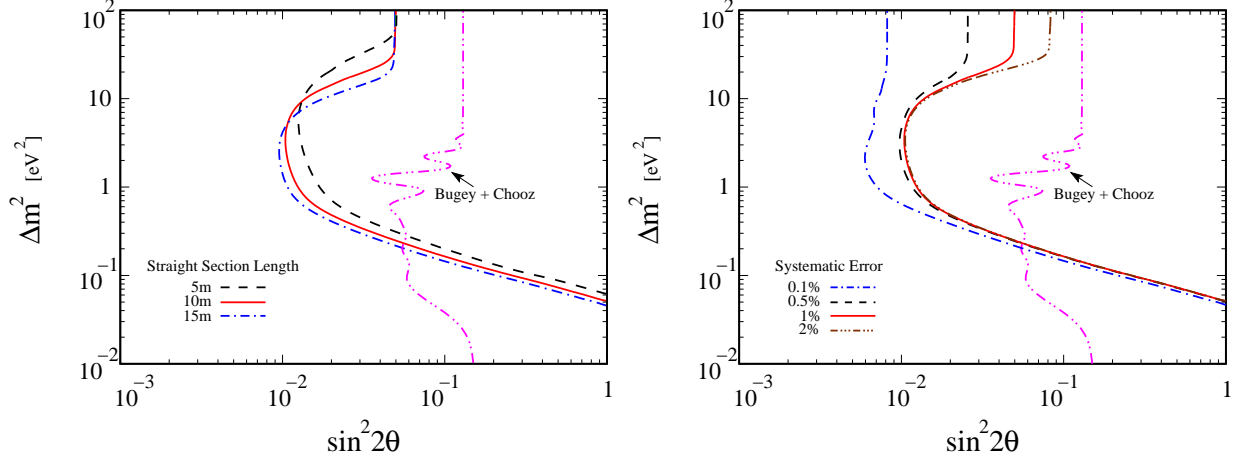


**FIG. 4:** Exclusion plots of sensitivity to active-sterile oscillations in a near detector low energy beta-beam set-up. These are 99% CL limits (1 dof). In left panel, we vary the straight section of the storage ring while in the right panel, we show the performance taking various values of expected systematic error of the considered setup. The pink (dash-dot-dotted line) line shows the current, combined limit on  $1 - P_{e\bar{e}}$  from Bugey [18] and Chooz [19].

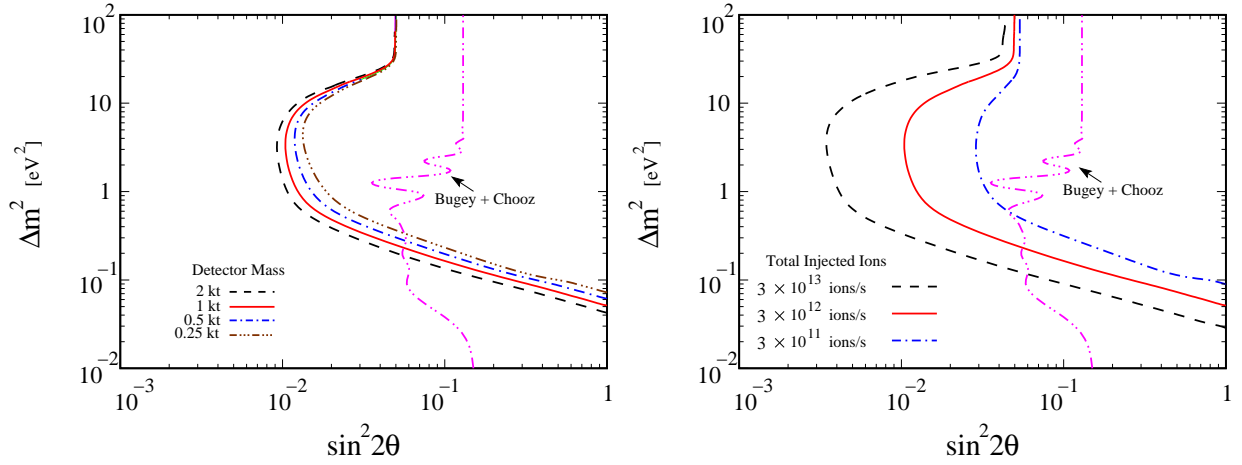


**FIG. 5:** Exclusion plots of sensitivity to active-sterile oscillations in near detector low energy beta-beam set-up. These are 99% CL limits (1 dof). In left panel, we choose different values of detector mass in the range 0.25 to 2 kton. Right panel depicts the performance of the set-up for different values of total injected ions. The pink (dash-dot-dotted) line shows the current, combined limit on  $1 - P_{e\bar{e}}$  from Bugey [18] and Chooz [19].

$\pi^s$  in the range  $0.005 - 0.05$  the sensitivity limit does not change for  $\Delta m^2 \leq 10 \text{ eV}^2$ , which is due to the cancellation of the normalization error between different oscillation maxima. This is also illustrated in figure 3.

Figure 5 shows the obtainable sensitivity in the  $\sin^2 2\theta - \Delta m^2$  plane at 99% CL. Our default configuration is shown as red solid line in both panels. The left hand panel shows how a variation of detector mass by a factor of 10 changes the sensitivity. Remarkably, this change is quite small: the detector density and aspect ratio are fixed. Thus with increasing detector

mass, the additional detector mass will be exposed to a weaker neutrino flux for purely geometrical reasons. The right hand panel shows the change of sensitivity for a changing beam luminosity and here the effect is quite pronounced as every additional ion contributes equally to improve the sensitivity. Note, the our default beam luminosity of  $3 \cdot 10^{12}$  ions  $s^{-1}$  is based on existing technology and thus may be somewhat conservative.

#### IV. CONCLUSIONS

We have studied a near detector setup at a low- $\gamma$  beta-beam facility for its ability to constrain the disappearance of electron anti-neutrinos for mass squared differences  $\Delta m^2 = 1 - 10 \text{ eV}^2$ . The key point is, that for a suitably chosen geometry several oscillation maxima occur within the same detector and thus a disappearance measurement at the sub-percent level becomes possible without requiring a stringent control on systematic errors. We focused on using a beam from the decay of  ${}^6\text{He}$ , which produces electron anti-neutrinos. This allows to use inverse beta decay as detection reaction and we can exploit the well defined relationship between the positron and neutrino energy. Thus, we have a very clean sample of electron anti-neutrino events. We carefully optimized the geometry and beam energy and found that  $\gamma = 30$  yields the best sensitivity while still having the bulk of neutrinos below the pion production threshold. In order to have sufficient resolution in  $L/E$  we had to reduce the length of the straight section down to 10 m, which makes this setup unique. Note, that this allows our experiment to run parasitically in a low energy beta-beam facility since we use only around 3% of all ions. Such a low energy beta-beam facility has been discussed extensively in the context of using neutrino nucleon scattering for studies of nuclear structure, see *e.g.* [16]. For a conservative beam luminosity of  $3 \cdot 10^{12}$  ions  $s^{-1}$  and detector mass of 1 kton we obtain a sensitivity to  $\sin^2 2\theta \simeq 10^{-2}$  (99% CL) for  $\Delta m^2 = 1 - 10 \text{ eV}^2$ .

#### Acknowledgments

SKA would like to thank Debabrata Mohapatra for useful discussions. JML acknowledges support from the Department of Energy under contract DE-FG02-92ER40709.

- 
- [1] S. Abe *et al.* [KamLAND Collaboration], Phys. Rev. Lett. **100**, 221803 (2008).
  - [2] W. M. Yao *et al.* [Particle Data Group], J. Phys. G **33**, 1 (2006).
  - [3] M. Maltoni, T. Schwetz, M. A. Tortola and J. W. F. Valle, New J. Phys. **6**, 122 (2004).
  - [4] P. Minkowski, Phys. Lett. B **67**, 421 (1977).
  - [5] C. Athanassopoulos *et al.* [LSND Collaboration], Phys. Rev. Lett. **81**, 1774 (1998).
  - [6] M. Maltoni and T. Schwetz, Phys. Rev. D **76**, 093005 (2007).
  - [7] T. Schwetz, JHEP **0802**, 011 (2008); Y. Farzan, T. Schwetz and A. Y. Smirnov, JHEP **0807**, 067 (2008).
  - [8] A. A. Aguilar-Arevalo *et al.* [MiniBooNE Collaboration], Phys. Rev. D **78**, 012007 (2008).
  - [9] S. Hannestad and G. G. Raffelt, JCAP **0611**, 016 (2006); S. Dodelson, A. Melchiorri and A. Slosar, Phys. Rev. Lett. **97**, 04301 (2006).

- [10] A. Kusenko, arXiv:hep-ph/0609158.
- [11] A. Boyarsky, O. Ruchayskiy and M. Shaposhnikov, arXiv:0901.0011.
- [12] M. Cirelli, G. Marandella, A. Strumia and F. Vissani, Nucl. Phys. B **708**, 215 (2005).
- [13] G. C. McLaughlin, J. M. Fetter, A. B. Balantekin and G. M. Fuller, Phys. Rev. C **59** (1999) 2873.
- [14] N. Okada and O. Yasuda, Int. J. Mod. Phys. A **12**, 3669 (1997).
- [15] K. Enqvist, K. Kainulainen and M. J. Thomson, Nucl. Phys. B **373**, 498 (1992); X. Shi, D. N. Schramm and B. D. Fields, Phys. Rev. D **48**, 2563 (1993); S. M. Bilenky, C. Giunti, W. Grimus and T. Schwetz, Astropart. Phys. **11**, 413 (1999); P. Di Bari, Phys. Rev. D **65**, 043509 (2002) [Addendum-ibid. D **67**, 127301 (2003)].
- [16] C. Volpe, J. Phys. G **30**, L1 (2004); G. C. McLaughlin and C. Volpe, Phys. Lett. B **591**, 229 (2004); G. C. McLaughlin, Phys. Rev. C **70** (2004) 045804; J. Serreau and C. Volpe, Phys. Rev. C **70**, 055502 (2004); A. B. Balantekin, J. H. de Jesus and C. Volpe, Phys. Lett. B **634**, 180 (2006); A. B. Balantekin, J. H. de Jesus, R. Lazauskas and C. Volpe, Phys. Rev. D **73**, 073011 (2006); N. Jachowicz and G. C. McLaughlin, Phys. Rev. Lett. **96**, 172301 (2006); P. S. Amanik and G. C. McLaughlin, Phys. Rev. C **75**, 065502 (2007); N. Jachowicz, G. C. McLaughlin and C. Volpe, Phys. Rev. C **77**, 055501 (2008).
- [17] S. M. Bilenky, C. Giunti and W. Grimus, Eur. Phys. J. C **1**, 247 (1998) [arXiv:hep-ph/9607372].
- [18] Y. Declais *et al.*, Nucl. Phys. B **434**, 503 (1995).
- [19] M. Apollonio *et al.* [CHOOZ Collaboration], Eur. Phys. J. C **27**, 331 (2003).
- [20] C. Grieb, J. Link and R. S. Raghavan, Phys. Rev. D **75**, 093006 (2007).
- [21] P. Zucchelli, Phys. Lett. B **532**, 166 (2002).
- [22] H. L. Ravn, *In the Proceedings of 16th IEEE Particle Accelerator Conference (PAC 95) and International Conference on High-energy Accelerators (IUPAP), Dallas, Texas, 1-5 May 1995, pp 858-863.*
- [23] M. Lindroos, Nucl. Phys. Proc. Suppl. **155**, 48 (2006).
- [24] <http://beta-beam-parameters.web.cern.ch/beta-beam-parameters/>
- [25] P. Vogel and J. F. Beacom, Phys. Rev. D **60**, 053003 (1999).
- [26] P. Huber, M. Lindner and W. Winter, Nucl. Phys. B **645**, 3 (2002).
- [27] G. L. Fogli, E. Lisi, A. Marrone, D. Montanino, A. Palazzo and A. M. Rotunno, Phys. Rev. D **67**, 073002 (2003).
- [28] A. A. Aguilar-Arevalo *et al.* [MiniBooNE Collaboration], Nucl. Instrum. Meth. A **599** (2009) 28.